

Physical characteristics and mechanical behaviour of maize stalks for machine development

Ádám Kovács* and György Kerényi

Department of Machine and Product Design, Budapest University of Technology and Economics, 3. Műgyetem rkp.,
Budapest, H-1111, Hungary

Received September 14, 2018; accepted April 23, 2019

Abstract. In order to optimize the design and working parameters of agricultural machinery related to harvesting, knowledge about the physical properties and mechanical behaviour of harvest-ready maize is required. Previous studies have been conducted on different maize varieties from different parts of the world in different growing seasons. However, these experiments were usually conducted on dried or deep-frozen samples and therefore the condition of these samples was not related to the harvested material. In order to produce more relevant experimental results, a complex measurement method that involves in-situ observations and laboratorial experiments was established after taking into consideration the process of maize harvesting with a combine harvester and a maize header. The measurement method was successfully conducted over a period of days of harvesting in Hungary. With regard to the physical properties of the stalk, the distribution of the internodal diameter and the length, mass and moisture content of the stalk were determined. The mechanical behaviour of the stalk was analysed through transversal compression, three-point bending and dynamic cutting experiments. The results clearly demonstrate that the physical properties (diameter, length and wet-mass ratio, moisture content) and mechanical properties (force response characteristic and required mechanical work) of different parts of the maize stalk vary significantly. Therefore, different parts of the maize stalk require different considerations during machine development.

Keywords: maize stalk, measurement method, mechanical behaviour, physical properties

INTRODUCTION

Maize (*Zea mays* L.) is one of the most cultivated crops in the world: almost 1100 million tonnes of maize were produced in 2017. Harvesting is one of the most crucial phases in maize production because the efforts invested over the

course of the whole growing season lead up to it, while the level of energy usage is relatively high. In order to optimize the machinery related to harvesting, knowledge concerning the physical characteristics and mechanical behaviour of maize is required.

During harvesting by a combine harvester, maize is mainly processed by the maize header; only maize ears are threshed inside the machine. The whole plant is cut and pulled down to gather the maize ears that are conveyed into the machine, while the rest of the maize plant (stalk, leaves, husk, tassel) is chopped. The wet mass of the stalks is more significant than the wet mass of the leaves, husk and tassel (Igathinathane *et al.*, 2006), moreover, it provides considerable resistance against external loads during processing, thus, it was selected for particular consideration in the current study.

To prevent spoilage and obtain comparable results, the moisture content of the specimens was usually reduced to 10-20% w.b. (Igathinathane *et al.*, 2010; Robertson *et al.*, 2014; 2015b) or adjusted to the predetermined values (*e.g.* 15-30-55-75% w.b.) (Ince *et al.*, 2005; Zhen *et al.*, 2013). Sometimes the specimens were stored in a deep-freezer (-25°C) until the experiments took place (Igathinathane *et al.*, 2011). Less frequently, virgin samples were investigated (Prasad and Gupta, 1975; Tongdi *et al.*, 2011).

Most of the previous studies focused on the geometrical (Robertson *et al.*, 2015a; Forell *et al.*, 2015), the chemical (Akgül *et al.*, 2010) and the structural (Heckwolf *et al.*, 2015; Huang *et al.*, 2016) properties of the stalks which have a significant influence on its mechanical behaviour.

*Corresponding author e-mail: kovacs.adam@gt3.bme.hu
kovadam19@gmail.com

The mechanical behaviour and breakage of agricultural or forestry materials are most commonly defined by compression (Prasad and Gupta, 1975; Robertson *et al.*, 2015b; Leblicq *et al.*, 2016; Zhang *et al.*, 2017), bending (Kantay *et al.*, 2000; Tongdi *et al.*, 2011; Robertson *et al.*, 2014, 2015b; Leblicq *et al.*, 2015; Olmedo *et al.*, 2016; Zhang *et al.*, 2017) and laboratorial cutting (Prasad and Gupta, 1975; O'Dogherty, 1982; Kantay *et al.*, 2000; Yiljep and Mohammed, 2005; Igathinathane *et al.*, 2009, 2010, 2011; Dange *et al.*, 2011; Johnson *et al.*, 2012; Kattenstroth *et al.*, 2012; Jia *et al.*, 2013; Mathanker *et al.*, 2015) experimental methods. In the case of the transversal compression and the three-point bending experiments, all of the previous experiments were quasi-static, and the deflection of the specimens was usually in the elastic state. One of the most effective ways to carry out the laboratorial dynamic cutting experiments on stalks and stems is the modification of a common pendulum impact machine (Azadbakht *et al.*, 2004; Yiljep and Mohammed, 2005; Dange *et al.*, 2011).

Based on a literature review, the previous experiments were usually conducted on dried or deep-frozen samples, therefore, the condition of these samples was not related to the harvested material. Moreover, the mechanical behaviour of the samples was estimated through small deformation loading cases, while a large deformation of the samples occurs during harvesting by a combine harvester with a maize header.

Therefore, the general objective of the current study is to determine the physical properties (diameter, length, mass and moisture content distribution) and mechanical properties (force response, required mechanical work distribution and breakage) of maize stalk as related to harvesting by a combine harvester. In order to achieve this goal, some specific objectives are defined as follows:

- first, a complex measurement method needs to be established by considering the usage of a universal testing machine to provide the applicability of the method in a common laboratory setting;
- second, the measurement method should be conducted during the harvesting period to provide data relevant to the harvested material;
- finally, the collected data needs to be analysed in such a way as to obtain useful knowledge about the condition and behaviour of the harvested material for machine development.

MATERIALS AND METHODS

Maize, of variety Sufavor FAO360 (Saaten-Union Hungária Ltd, Hungary), was planted in the central region of Hungary (location: 47°44' N; 19°36' E, 149 m a.s.l.) on 15 April 2016. The plant density was 70000 units ha⁻¹ and the distance between the rows and plants was 0.75 and 0.2 m, respectively. The ears were harvested on 26-27 October

2016, when the average moisture content of the threshed maize kernels was 19.7% w.b. and the yield was 8800 kg ha⁻¹.

For all of the tests, healthy plants without any observable damage, disease or mutation were systematically selected to facilitate uniform sample collection. In-situ observation was conducted on virgin samples at the experimental plot. For the laboratory tests, samples were cut right above the soil surface and transported to the laboratory.

According to the in-situ observation of 100 plants, the upper part of the stalk was broken or completely missing for 93% of the samples. To provide comparable results, experiments on the first ten internodes and nodes were conducted.

Before the experiments, the nodes (N) and internodes (IN) of each stalk were continuously numbered and marked by position indices (p) from the bottom to the top of the stalk (1, 2, ..., 10). The stump, where the brace root joins the stalk, was excluded from the measurement because this part does not come into contact with the maize header.

Afterwards, the stalks were cut into smaller samples by a bandsaw and they were measured within 8 h after collection during harvesting days on 26-27 October 2016. Therefore, the properties of the stalks remained close to their condition during harvest.

In the laboratory, the minor and major dimensions of nodal and internodal cross-sections were measured on 10 stalks using a digital calliper (accuracy 0.01 mm). Along the internodal sections, the equivalent diameter was assumed to be constant (Robertson *et al.*, 2015a). Thus, these dimensions were measured in one cross-section near to the middle of the section. The distance between the two nodes (length of the internodes) was also measured on 10 stalks by using a measuring tape (accuracy 1 mm).

Ten stalks were cut into internodal sections using a bandsaw and the wet-mass of internodes was measured using a digital balance (accuracy 0.01 g). Afterwards, the same internodes were placed into a drying oven at 102°C and the dry-mass of the internodes was measured after 24 h (Igathinathane *et al.*, 2006).

The complex cross-sectional shape of the real internode and node was approximated by an equivalent circular cross-section (Igathinathane *et al.*, 2006). The equivalent diameter ($d_{ep}^{IN/N}$) was calculated by using the width of the real cross-section in the major (w_p^{mj}) and minor directions (w_p^{mr}) in Eq. (1):

$$d_{ep}^{IN/N} = \frac{w_p^{mj} + w_p^{mr}}{2}. \quad (1)$$

For each stalk, all of the equivalent diameters were specified by using the equivalent diameter of the first node (d_{e1}^N) in Eq. (2):

$$\delta_p^{IN/N} = \frac{d_{ep}^{IN/N}}{d_{e1}^N}, \quad (2)$$

where: $\delta_p^{IN/N}$ (-) is the equivalent diameter ratio of the circular cross-section.

The measured length of the internodes (L_p) were specified by the total length of the stalk (L_t), see Eq. (3):

$$\lambda_p = \frac{L_p}{L_t}, \quad (3)$$

where λ_p (-) is the internodal length ratio.

Each measured wet-mass ($m_{w,p}$) was specified by the total wet-mass of the stalk ($m_{w,t}$), see Eq. (4):

$$\mu_{w,p} = \frac{m_{w,p}}{m_{w,t}}, \quad (4)$$

where $\mu_{w,p}$ (-) is the internodal wet-mass ratio.

The moisture content of the internode (MC_p) was calculated based on the measured internodal wet-mass ($m_{w,p}$) and dried-mass ($m_{d,p}$) as specified by Eq. (5):

$$MC_p = \frac{m_{w,p} - m_{d,p}}{m_{w,p}} \cdot 100. \quad (5)$$

Generally, all of the mechanical experiments in the current study focus on the internodal sections of the stalk because the likelihood of loading on an internodal section of the stalk is higher than on the nodal section (Igathinathane *et al.*, 2011). Before the experiments, the minor and major dimensions of the internodal cross-section were measured for each sample by using a digital calliper (accuracy 0.01 mm). During all of the experiments, the minor axis of the internodes was in the direction of the load, therefore displacement data were collected at 100 Hz by a universal testing machine (Zwick Z020 test frame with a 5000-N load cell) and high-resolution videos were recorded for each sample at a rate of 30 frames per second. Afterwards, the recorded videos and force-displacement curves were analysed in detail to determine the mechanical behaviour of the stalks, moreover, in order to analyse the required compressive and bending work requirement of the internodal sections Eq. (6) may be used:

$$W = \sum_{i=1}^n \frac{F_i + F_{i+1}}{2} \times (s_{i+1} - s_i), \quad (6)$$

where: W (J) is the required compressive or bending work, F (N) is the force response at any instant, s (m) is the displacement of the plunger at any instant.

Transversal compression between flat plates was conducted on each internode of 10 maize stalks with a deformation speed of 300 mm min^{-1} (Fig. 1a). For the sectional transversal compression test, samples with a 50 mm length were cut from the middle section of internodes. First, the plunger approached the sample with a velocity of 10 mm min^{-1} until reaching a preload of 2 N. For all of the investigated internodes, the applied preloads provide full-contact among the plungers and both sides of the sample. The minor width of the sample (w_p^{mr}) was recorded after the preload

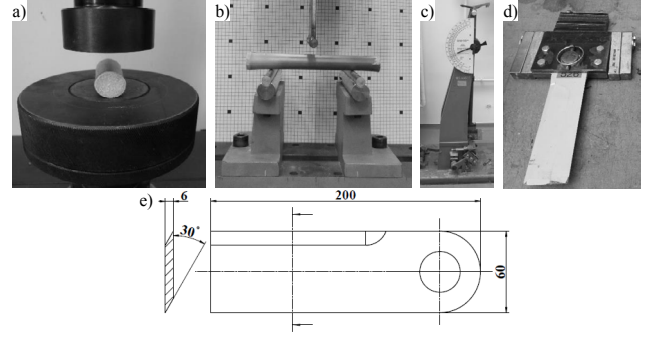


Fig. 1. Experiments: a) transversal compression, b) three-point bending, c) pendulum impact machine, d) cutting blade unit for dynamic cutting, e) design of the cutting blade (all dimensions in mm).

force was applied and compression was then carried out until 0.75 of the compression rate (κ) of the samples was reached, that value was calculated using Eq. (7):

$$\kappa = \frac{s}{w_p^{mr}}. \quad (7)$$

Three-point bending experiments on each internode of 10 maize stalks were conducted with a deformation speed of 300 mm min^{-1} , while the bending tool and the supports had a cylindrical shape with a diameter of 10 mm (Fig. 1b). In contrast to the results of the previous studies (Robertson *et al.*, 2014) a span length of 100 mm was chosen and the samples were loaded into the middle of the internodal sections. This adjustment of the span length resulted in a loading profile similar to that which actually occurs during harvesting. For all the samples, the displacement of the bending tool was 30 mm. First, the bending tool approached the samples with a velocity of 10 mm min^{-1} until it reached a preload value of 2 N.

A pendulum impact machine (Métisz-Q Ltd, type WPM 406/60/18, Fig. 1c) was modified by replacing the hammer with the cutting blade unit of a harvester (Fig. 1d) in such a way that the gap between the blade (Fig. 1e) and the supports was approximately 6 mm on both sides. The cutting test was carried out on each internode of 10 maize stalks. Without causing local deformation, the samples were fixed at both ends to cut them along their minor axis. The pendulum started from the same position each time. Therefore, the cutting velocity of the blade unit was 3.5 m s^{-1} in every case. The reversal angle was visualized and recorded with a scale. Based on the recorded data, the required dynamic cutting work (W^{DC}) was calculated using Eq. (8):

$$W^{DC} = m \times g \times l \times (\cos \beta - \cos \alpha), \quad (8)$$

where: m (kg) is the mass of the swinging part, g (m s^{-2}) is the gravitational acceleration, l (m) is the distance of the centre of the gravity of the swinging part from the pivot point of the pendulum, β ($^\circ$) is the maximum angle of deflection on the pendulum after the cutting is complete

and α ($^\circ$) is the maximum angle of deflection on the pendulum before the cutting process was initiated. The α and β angles were recorded by visual reading, thus, the reading error was approximately 1° .

For further analysis, the calculated, required cutting work (W^{DC}) was specified by the cross-sectional area of the internode, using Eq. (9):

$$\omega^{DC} = \frac{W^{DC}}{\frac{(d_e^{IN})^2 \times \pi}{4}}, \quad (9)$$

where: ω^{DC} (J mm $^{-2}$) is the specific required dynamic cutting work and d_e^{IN} (mm) is the equivalent diameter of the internode.

RESULTS

All of the results obtained are reported in the form expressed by Eq. (10):

$$\bar{X} \pm CI, \quad (10)$$

where: \bar{X} is the mean of the measured variable, and CI is the radius of the confidence interval at a 5% significance level ($p = 0.05$).

The measured mean equivalent diameter of the first node (d_{e1}^N) was 28.5 ± 1.4 mm. The characteristics of the mean nodal and internodal equivalent diameter ratios vs position indices showed a strong correlation ($R = 0.99$, $R = 0.98$) (Fig. 2a). For the nodes, the inflection point of the bilinear characteristic is situated at the sixth nodal position index (where the maize ear was situated), while, for the internodes it was situated at the fifth internodal position index (right below the maize ear).

The measured mean total length of the first ten internodes was 1510 ± 128 mm. Three phases were determined based on the characteristics of the internodal length ratios vs position indices (Fig. 2b): the length ratio is linearly increasing between the first and the fourth internodes, where it reaches a maximum value; afterwards, it starts to linearly decrease until it reaches a constant value at the ninth internode.

The measured mean wet-mass of the first ten internodes was 191.7 ± 38.5 g. The wet-mass ratio of the internodes decreases significantly from the first to the fifth internode

where the gradient of decrease drops (Fig. 2c). The mean moisture content of the internodes decreases linearly from the first to the eighth internode, where it starts to decrease more significantly (Fig. 2c).

The typical phases of the force response were determined based on the measured characteristics during transversal compression (TC) experiments (Fig. 3).

For most of the internodal positions (2nd-5th and 7th) the characteristics were made up of the same phases (Fig. 3b): an initial quasi-linear increasing phase; one significant initial break and then an exponential increase with small drops. In the case of the first internode, multiple breaks with increasing linear phases may be observed after the initial increase (Fig. 3a). Only in the case of the sixth internode, was the initial quasi-linear increasing phase followed by a quasi-constant phase (Fig. 3c). The typical characteristics of the eighth and ninth internodes contained the same phases (Fig. 3d, e), however, the position of the initial break was significantly different. Moreover, the initial break was not observable in the case of the tenth internode (Fig. 3f).

Through an analysis of the relationship between the maximal compressive force at the 0.75 compression rate (F_{max}^{TC}) and the equivalent diameter of the internodes (d_e^{IN}), a strong correlation ($R = 0.92$) was found, as shown in Fig. 4(a), and an exponential relationship was determined, see Eq. (11):

$$F_{max}^{TC} = 360.98 \times e^{0.099 \times d_e^{IN}} (R^2 = 0.87). \quad (11)$$

The required mean compressive work ($\overline{W^{TC}}$) distribution on the maize stalks is shown in Fig. 3b. The results showed that the mean required compressive work significantly decreases up to the top of the stalk and the first five internodes provided 77.8% (42.6 J) of the total required compressive work (54.8 J) on an average stalk.

Through an analysis of the compressive work (W^{TC}) required and the internodal equivalent diameter (d_e^{IN}), a close correlation ($R = 0.93$) was found (Fig. 4c), and an exponential relationship was determined (Eq. (12)):

$$W^{TC} = 0.506 \times e^{0.1402 \times d_e^{IN}} (R^2 = 0.95). \quad (12)$$

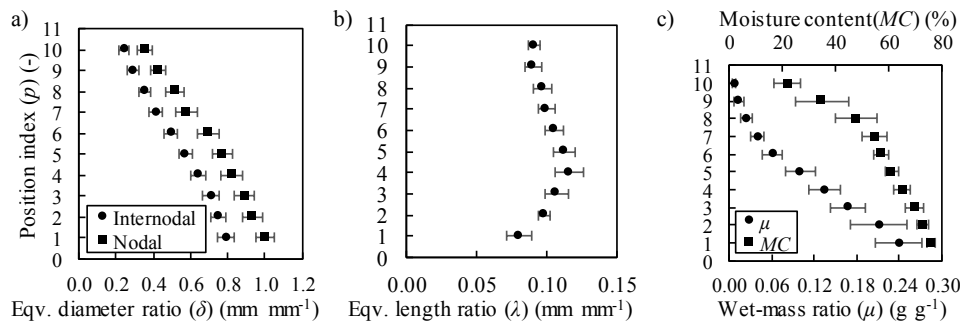


Fig. 2. Physical characteristics of maize stalks; a) mean equivalent diameter ratio distribution of the internodes and the nodes of maize stalks; b) mean length ratio distribution of the internodes of maize stalks and c) mean wet-mass ratio and mean moisture content distribution of the internodes of maize stalks (error bars represent the confidence interval (CI) at the 5% significance level ($p = 0.05$)).

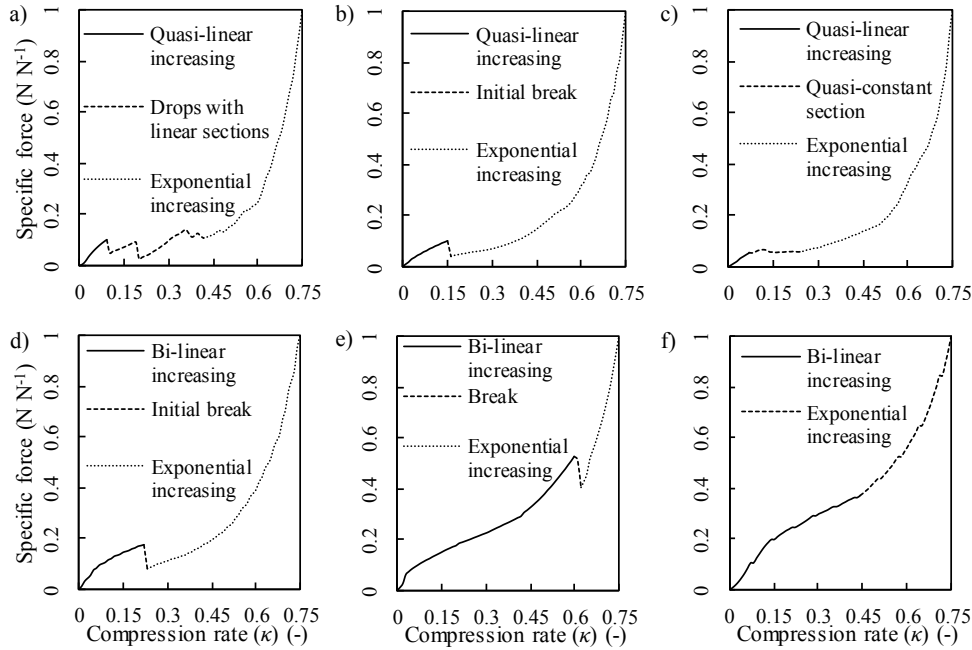


Fig. 3. Typical phases of specific force – compression rate curves of transversal compression experiments on the internodes: a) typical characteristics for the first internodes, b) typical characteristics for the 2nd-5th and 7th internodes, c) typical characteristics for the sixth internode, d) typical characteristics for the eighth internode, e) typical characteristics for the ninth internode, and f) typical characteristics for the tenth internode.

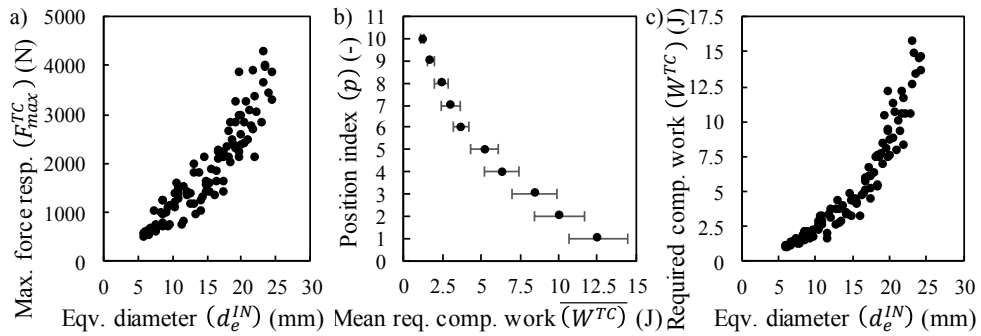


Fig. 4. Maximal compressive force and required work by transversal compression: a) relationship between the maximal compressive and the equivalent diameter of the internodes; b) mean required compressive work distribution of the maize stalk, the error bar represents the confidence interval (CI) at the 5% significance level ($p = 0.05$) and c) the relationship between the required compressive work and the equivalent diameter of internode.

During an analysis of the recorded videos, five major phenomena could be observed: ovalization, the vertical break of the core, the vertical break of the rind, horizontal breaks of the rind and flattening. Moreover, most of them were related to the measured force response, as shown in Fig. 4. At the beginning of the compression, the sample was ovalized without any observable damage or break in its structure, this was related to the initial, quasi linear increasing phase (Fig. 5a). After that, a straight vertical break appeared in the core of the sample in relation to one significant, initial break phase (Fig. 5b). The vertical break of the core propagated to the rind while the sample broke into two separated parts (Fig. 5c). On both sides of the rind, small breaks appeared in the horizontal direction and these

breaks propagated to the boundary between the rind and the core resulting in small drops in the exponentially increasing phase (Fig. 5d). After the structural collapse of the rind, the core had a more significant effect on the mechanical behaviour of the maize stalks against transversal compression (Fig. 5e).

In the case of the three-point bending (TB) experiment, the bending characteristic may be divided into four typical phases: an initial elastic phase where the force response increases linearly; a plastic phase where the force-displacement curve reaches its peak; the phase of structural collapse (buckling) where the force response decreases until it reaches an ultimate value and the sliding phase where the force response remains constant, as shown in Fig. 6a.

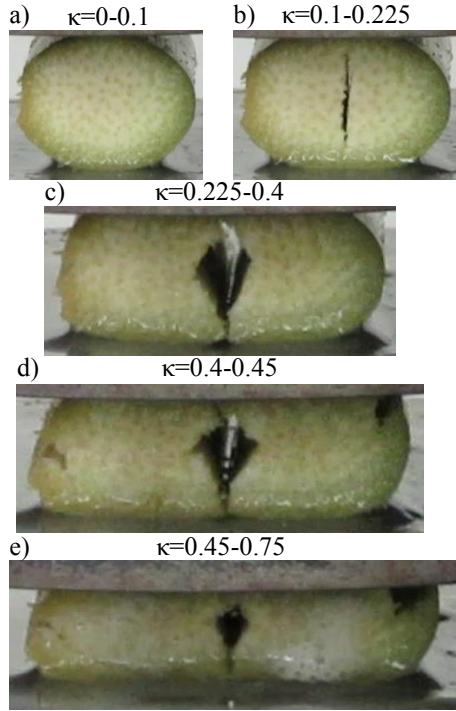


Fig. 5. Major breaking phenomena of the internodal sections during compression: a) ovalization, b) vertical break of the core, c) vertical break of the rind, d) horizontal breaks of the rind and e) flattening.

Figure 6b shows the mean peak and mean ultimate force values for each internodal section. A close correlation was found between the position indices, the mean peak ($r=-0.94$) and the mean ultimate ($R = -0.95$) forces. These relationships were determined by Eqs (13), (14):

$$\overline{F_p^{TB}} = 612.75 \times e^{-0.373 \times p} \quad (R^2 = 0.96), \quad (13)$$

$$\overline{F_U^{TB}} = -106.2 \times \ln(p) + 238.19 \quad (R^2 = 0.99). \quad (14)$$

The mean displacement of the plunger where the peak force appears (DoP) and the mean ratio between the peak and the ultimate forces ($\phi_{p,U}^{TB}$) are shown in Fig. 6c. A strong correlation ($R = -0.96$) was found between the DoP and the position indices (p) of the stalk and a linear relationship was defined by Eq. (15):

$$\text{DoP}_{p=1-10} = -0.4152 \times p + 8.2333 \quad (R^2 = 0.92). \quad (15)$$

The mean ratio between the peak and the ultimate forces were divided into two sections: under and above the position of the maize ear. Under the maize ear the mean ratio was nearly constant, while above the maize ear it increased linearly (Eqs (16), (17)):

$$\phi_{p,U}^{TB} \quad (p=1-6) = 1.6383, \quad (16)$$

$$\phi_{p,U}^{TB} \quad (p=7-10) = 0.8160 \times p - 3.15 \quad (R^2 = 0.99). \quad (17)$$

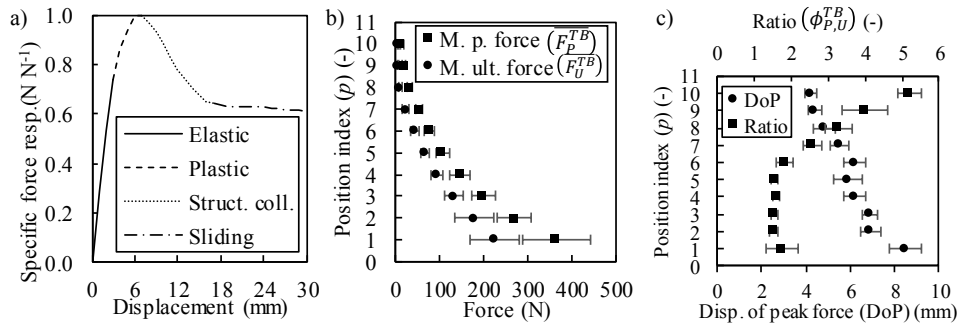


Fig. 6. Typical force response characteristics of the three-point bending experiment on internodes: a) typical phases of the curve, b) distribution of the mean peak and mean ultimate forces and c) distribution of the mean displacement of the peak force and distribution of the mean ratio between the peak and the ultimate forces (error bars represent the confidence interval (CI) at the 5% significance level ($p = 0.05$)).

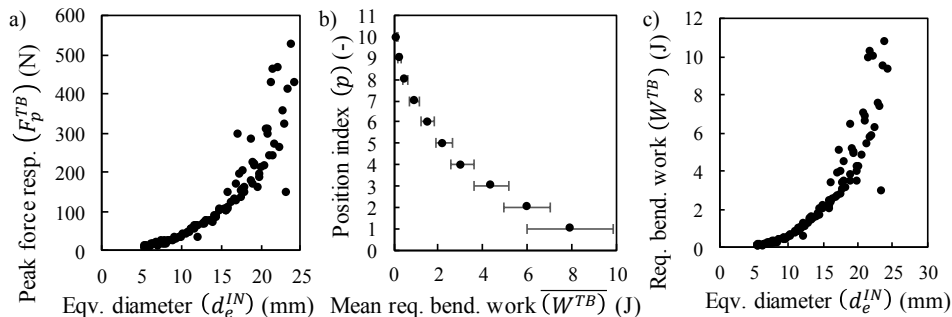


Fig. 7. Peak force and bending work characteristics of the three-point bending experiments: a) relationship between the peak forces and the equivalent diameter of the internodes, b) mean required bending work distribution on a maize stalk, the error bar represents the confidence interval (CI) at the 5% significance level ($p = 0.05$) and c) the relationship between the required bending work and the equivalent diameter of the internode.

Through further analysis of the peak force and the equivalent diameter of the internode, a close correlation ($r = 0.89$) was found (Fig. 7a), and an exponential relationship was determined (Eq. (18)):

$$F_p^{TB} = 0.0818 \times e^{2.6432 \times d_e^{IN}} \quad (R^2 = 0.96) \quad (18)$$

The mean required bending work ($\overline{W^{TB}}$) distribution on the maize stalks is shown in Fig. 7b. The results showed that it decreases significantly from the bottom to the top sections of the stalk and the first five internodes provided 87.4% (23.62 J) of the total required bending work (27.04 J) on an average stalk.

Through an analysis of the required bending work ($\overline{W^{TB}}$) and the internodal equivalent diameter (d_e^{IN}), a close correlation ($R = 0.89$) was found (Fig. 7c), and an exponential relationship was determined (Eq. (19)):

$$W^{TB} = 0.0459 \times e^{0.2376 \times d_e^{IN}} \quad (R^2 = 0.94) \quad (19)$$

The damage and breaking phenomena of the samples were analysed based on the high-resolution records (Fig. 8). The following major phenomena could be observed: ovalization (flattening), structural collapse (buckling), sliding and residual deformation. These phenomena were also related to the typical phases of the resistance force – displacement curves of the three-point bending experiments. At the beginning of the bending phase, the cross-section under the bending tool was ovalized without any observable damage or break in the rind structure (Fig. 8a). This phenomenon took place in a small area near the bending tool and resulted in a flattened and ovalized cross-section, but real bending deformation did not occur instead it was a transversal deformation. This phenomenon relates to the elastic phase of the resistance force – displacement curve. The structure became unstable in the bending area and longitudinal breaks appeared which resulted in a plastic-hinge (structural collapse) under the bending tool (Fig. 8b). These breaks usually propagated to the ends of the specimen. This phenomenon relates to the structural collapse phase of the force response. At the end of the process, the sample slid on the supports while it provided constant resistance against bending, as shown in Fig. 8c). After the experiments, the cross-sections in the bending area had a residual deformation (Fig. 8d). In the case of the drier samples, the significance of the residual deformation was higher.

The mean dynamic cutting work required decreases as the position index increases, but two different stages were observable (Fig. 9a). Above the fifth internode, a significant drop may be observed in the characteristic while the gradation of the decreases were nearly the same. The mean required cutting work on the first internode (21.13 J) was 7 times higher than on the tenth internode (3.02 J) and the first five internodes provided 78.8% (90.4 J) of the total required cutting work (114.7 J) on an average stalk.

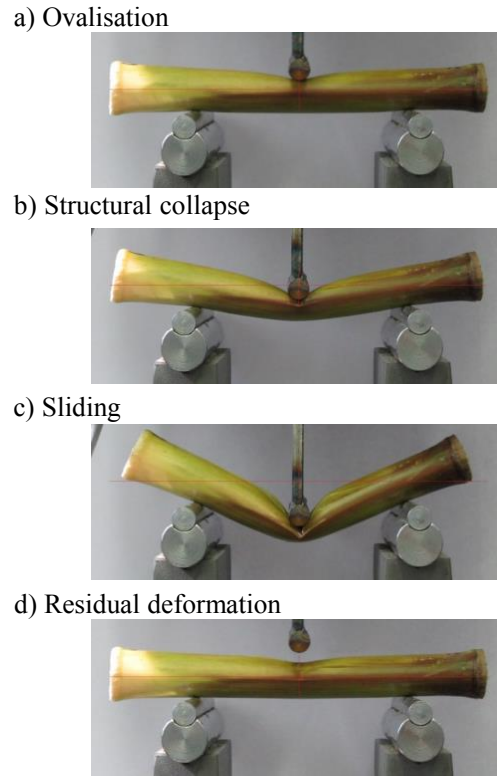


Fig. 8. Typical damage and breaking phenomena of the samples during the three-point bending experiments: a) ovalization (flattening), b) structural collapse, c) sliding, d) residual deformation.

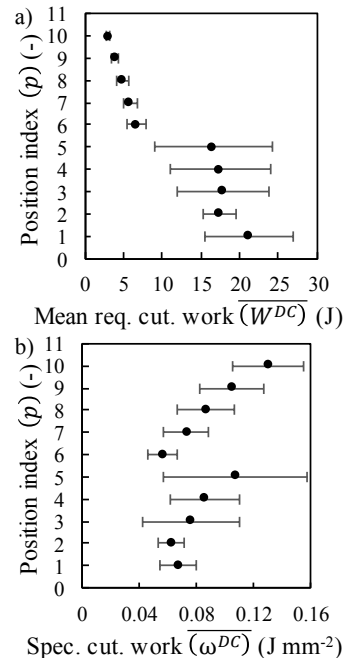


Fig. 9. Required dynamic cutting work: a) mean required work distribution and b) mean specific required cutting work distribution on a maize stalk, the error bar represents the confidence interval (CI) at the 5% significance level ($p = 0.05$).

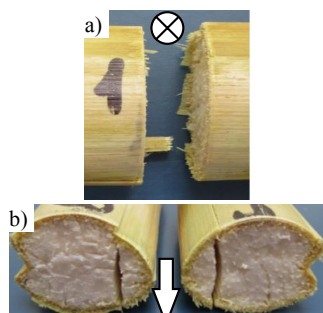


Fig. 10. Typical surfaces of a cut: a) rim of fibres on the side where the cutting knife left the sample and b) breaks in the cross-section perpendicular to the direction of the cut.

The mean specific required dynamic cutting work vs the position of the internode on the stalk is shown in Fig. 9b. The mean values were nearly the same for the first two internodes but after that they increase until they reach the fifth internode, where a significant drop may also be observed. Above the sixth internode the mean specific required dynamic cutting work increases linearly.

The damage to the samples was analysed after the cutting process of the experiments (Fig. 10). A significant break perpendicular to the cutting direction appeared, while the surface of the cut was perfectly straight. However, a rim of fibres was usually observed on the side where the cutting blade left the sample.

DISCUSSION

The results clearly demonstrate that the physical properties and mechanical behaviour of different parts of the maize stalk vary significantly. Therefore, different parts of the maize require different approaches during machine development.

The results of previous studies show the same linear relationship between the equivalent diameters of the internodes and their positions on the maize stalks (Igathinathane *et al.*, 2006; Robertson *et al.*, 2015a; Huang *et al.*, 2016), moreover, a similar equivalent length ratio characteristic was determined in relation to sorghum stalks (Bakeer *et al.*, 2012). A similar wet mass and moisture content distribution on the stalk was also reported by Igathinathane *et al.* (2006). The sum of the wet-mass ratios of the first five internodes was 0.85, therefore, the total wet-mass of the internodes under the maize ear was more significant with regards to biomass production. The lower moisture content in the upper parts of the stalk results in a more brittle behaviour under external loading, this is the reason for the broken or missing upper parts of the stalks which were observed at the experimental plot.

The determined force responses of the samples against transversal compression and three-point bending were also reported by Tongdi *et al.* (2011); Zhen *et al.* (2013); Leblicq *et al.* (2015); Zhang *et al.* (2017). Moreover, the range of

the mean peak bending force (146.62-364.24 N) and the mean displacement range of the peak bending force (6.2-8.5 mm) on the internodal sections from the 1st to the 4th correspond with the results obtained by previous studies (190.54-314.36 N; 4.31-10.16 mm) (Tongdi *et al.*, 2011).

In the case of the quasi-static cutting tests, the first stage of cutting is the compression stage (Igathinathane *et al.*, 2010) where the force response reaches its peak. The observed vertical break on the tested samples indicates that the first stage of the dynamic cut is also transversal compression. Moreover, the presence of a rim of fibres on the side where the cutting blade left the sample proves that the final cut of the internode (Igathinathane *et al.*, 2010) was not precise because of the additional bending effect.

The calculated ratio between the peak and the ultimate forces demonstrates the flexibility of the samples: in a more flexible maize stalk, the structural collapse under the bending tool does not lead to a rupture of the fibres, so they can support more of the structure against subsequent loads. It is well known that the flexibility of stalks depends on their moisture content. This explains why the ratio increases significantly above the position of the maize ear where the moisture content of the stalk decreases significantly as well and why it is quasi-constant under the position of the maize ear where the moisture content decreases slightly.

The maximal compressive force occurs at the 0.75 compression rate, the peak and ultimate bending forces decrease from the bottom to the top of the maize stalk. This relationship corresponds with previous results by Zhang *et al.* (2017) and Huang *et al.* (2016). Their results show that the bottom (root) section of the stalk, where the moisture content of the cellulose and the cross-sectional area are higher, provides a greater resistance against external load than the upper parts of the stalk (middle and top sections).

The required compressive, bending and cutting work of the internodal sections decreases significantly from the bottom to the top of the stalk. The current results show that the required work to compress, bend and cut the internodal sections under the maize ear provides the majority (77.8, 87.4, 90.4% for compression, bending and cutting, respectively) of the total required bending work on an average maize stalk and, therefore, the significance of these parts is higher than the upper parts of the stalk from the point of view of the energy consumption during processing.

Generally, the observed damage and breaking phenomena explain the force responses of the samples. In the case of three-point bending, the ovalization and buckling of the samples were also reported during three-point bending experiments on wheat (*Triticum* L.) and barley (*Hordeum vulgare* L.) stems (Leblicq *et al.*, 2015). Moreover, the crack propagation in the longitudinal direction of the internode during the structural collapse phase was also reported by Tongdi *et al.* (2011). Furthermore, the results of previous experiments on wheat, barley (Leblicq *et al.*, 2015) and maize (Robertson *et al.*, 2014) and the results

from the transversal compression and three-point bending experiment of the current study indicate that the core contributions to the compression and bending resistance of maize stems occur after the structural collapse of the rind.

CONCLUSIONS

1. The measurements performed on the physical properties of the stalk clearly demonstrate that there is a direct relationship between the position indices and the diameter ratio, length ratio, wet-mass ratio and moisture content, respectively.

2. Based on the experiments with the mechanical properties of the stalk, the mechanical resistance of the internodal sections decrease from the bottom to the top, moreover, the upper stalk parts are less flexible.

3. The quasi-linear increases, initial break, drops with linear phases and exponentially increasing phases of the typical force response are directly related to the breakage of the samples; ovalization, the vertical break of the core, the horizontal break of the skin and flattening; during the transversal compression experiments.

4. The elastic, plastic and structural collapse phases of the typical force response are directly related to the breakage of the samples; ovalization, the appearance of longitudinal breaks and the evolution of a plastic hinge; during the three-point bending experiments.

Conflict of interest: The Authors declare that they have no conflict of interest.

Compliance with ethical requirements: This study does not contain any experiment involving human or animal subjects.

REFERENCES

- Akgül M., Güler C., and Cöpür Y., 2010.** Certain physical and mechanical properties of medium density fiberboards manufactured from blends of corn (*Zea mays indurata* Sturt.) stalks and pine (*Pinus nigra*) wood. Turkish J. Agric. Forestry, 34, 197-206.
- Azadbakht M., Rezaei AA., and Zahedi KT., 2004.** Energy requirement for cutting corn stalks. Int. J. Biological, Veterinary, Agricultural and Food Engineering, 8(5), 467-470.
- Bakeer B., Taha I., El-Mously H., and Shehata S.A., 2013.** On the characterisation of structure and properties of sorghum stalks. Ain Shams Engineering J., 4, 265-271. <https://doi.org/10.1016/j.asej.2012.08.001>
- Dange AR., Thakare SK., and Rao I.B., 2011.** Cutting energy and force as required for Pigeon pea stems. Int. J. Agric. Technol., 7(6), 1485-1493.
- Forell G.V., Robertson D., Lee S.Y., and Cook D.D., 2015.** Preventing lodging in bioenergy crops: a biomechanical analysis of maize stalks suggests a new approach. J. Exp. Botany, 66(14), 4367-4371. <https://doi.org/10.1093/jxb/erv108>
- Heckwolf S., Heckwolf M., Kaeppler S.M., Leon N., and Spalding E.P., 2015.** Image analysis of anatomical traits in stalk transections of maize and other grasses. Plant Methods, 11, 26. <https://doi.org/10.1186/s13007-015-0070-x>
- Huang J., Liu W., Zhou F., Peng Y., and Wang N., 2016.** Mechanical properties of maize fibre bundles and their contribution to lodging resistance. Biosystems Eng., 151, 298-307. <https://doi.org/10.1016/j.biosystemseng.2016.09.016>
- Igathinathane C., Pordesimo L.O., Schilling M.W., and Columbus E.P., 2011.** Fast and simple measurement of cutting energy requirement of plant stalk and prediction model development. Industrial Crops and Products, 33, 518-523. <https://doi.org/10.1016/j.indcrop.2010.10.015>
- Igathinathane C., Womac A.R., and Sokhansanj S., 2010.** Corn stalk orientation effect on mechanical cutting. Biosystems Engineering, 107, 97-106. <https://doi.org/10.1016/j.biosystemseng.2010.07.005>
- Igathinathane C., Womac A.R., Sokhansanj S., and Narayan S., 2009.** Size reduction of high- and low-moisture corn stalks by linear grid system. Biomass Bioenerg., 33, 547-557. <https://doi.org/10.1016/j.biombioe.2008.09.004>
- Igathinathane C., Womac A.R., Sokhansanj S., and Pordesimo L.O., 2006.** Mass and Moisture distribution in aboveground components of standing corn plants. Am. Soc. Agric. Biol. Eng., 49(1), 97-106. <https://doi.org/10.13031/2013.20217>
- Ince A., Ugurluay S., Güzel E., and Özcan M.T., 2005.** Bending and shearing characteristics of sunflower stalk residue. Biosystems Eng., 92(2), 175-181. <https://doi.org/10.1016/j.biosystemseng.2005.07.003>
- Jia H., Li C., Zhang Z., and Wang G., 2013.** Design of bionic saw blade for corn stalk cutting. J. Bionic Eng., 10, 497-505. [https://doi.org/10.1016/s1672-6529\(13\)60242-5](https://doi.org/10.1016/s1672-6529(13)60242-5)
- Johnson P.C., Clementson C.L., Mathanker S.K., Grift T.E., and Hansen A.C., 2012.** Cutting energy characteristics of Miscanthus x giganteus stems with varying oblique angle and cutting speed. Biosystems Eng., 112, 42-48. <https://doi.org/10.1016/j.biosystemseng.2012.02.003>
- Kantay R., As N., and Ünsal Ö., 2000.** The mechanical properties of walnut (*Juglans regia* L.) wood. Turkish J. Agric. Forestry, 24, 751-756.
- Kattenstroth R., Harms HH., and Frerichs L., 2012.** Influence of the straw alignment on the cutting quality of combine's straw chopper. Landtechnik, 67(4), 244-246.
- Leblicq T., Smeets B., Ramon H., and Saeys W., 2016.** A discrete element approach for modelling the compression of crop stems. Computers and Electronics in Agriculture, 123, 80-88. <https://doi.org/10.1016/j.compag.2016.02.018>
- Leblicq T., Vanmaercke S., Ramon H., and Saeys W., 2015.** Mechanical analysis of the bending behaviour of plant stems. Biosystems Eng., 129, 87-99. <https://doi.org/10.1016/j.biosystemseng.2014.09.016>
- Mathanker SK., Grift TE., and Hansen AC., 2015.** Effect of blade oblique angle and cutting speed on cutting energy for energycane stems. Biosystems Eng., 133, 64-70. <https://doi.org/10.1016/j.biosystemseng.2015.03.003>
- O'Dogherty MJ., 1982.** A review of research on forage chopping. J. Agric. Eng. Res., (27), 267-289. [https://doi.org/10.1016/0021-8634\(82\)90068-3](https://doi.org/10.1016/0021-8634(82)90068-3)

- Olmedo I., Bourrier F., Bertrand D., Berger F., and Limam A., 2016.** Discrete element model of the dynamic response of fresh wood stems to impact. *Eng. Structures*, 120, 13-22. <https://doi.org/10.1016/j.engstruct.2016.03.025>
- Prasad J. and Gupta C.P., 1975.** Mechanical properties of maize stalk as related to harvesting. *J. Agric. Eng. Res.*, 20(1), 79-87. [https://doi.org/10.1016/0021-8634\(75\)90098-0](https://doi.org/10.1016/0021-8634(75)90098-0)
- Robertson D.J., Julias M., Gardunia B.W., Barten T., and Cook D.D., 2015a.** Corn stalk lodging: A forensic engineering approach provides insights into failure patterns and mechanisms. *Crop Science*, 55, 2833-2841. <https://doi.org/10.2135/cropsci2015.01.0010>
- Robertson D.J., Smith L.S., and Cook D.D., 2015b.** On measuring the bending strength of septate grass stems. *American J. Botany*, 102(1), 5-11. <https://doi.org/10.3732/ajb.1400183>
- Robertson D., Smith S., Gardunia B., and Cook D., 2014.** An improved method for accurate phenotyping of corn stalk strength. *Crop Science*, 54, 2038-2044. <https://doi.org/10.2135/cropsci2013.11.0794>
- Tongdi Q., Yaoming L., and Jin C., 2011.** Experimental study on flexural mechanical properties of corn stalks. *Chinese Book Classification*, No.: S225.3, 130-134. <https://doi.org/10.1109/icae.2011.5943766>
- Yiljep Y. and Mohammed U., 2005.** Effect of Knife Velocity on Cutting Energy and Efficiency during Impact Cutting of Sorghum Stalk. *Agric. Eng. International: the CIGR EJournal. Manuscript*, PM 05 004. Vol. VII.
- Zhang K., He Y., Zhang H., and Li H., 2017.** Research on mechanical properties of corn stalk. *AIP Conf. Proc.*, February 25-26, Wuhan, China.